

# Multipartite entanglement at dynamical quantum phase transitions with non-uniformly spaced criticalities

Stav Haldar<sup>1</sup>, Saptarshi Roy<sup>1</sup>, Titas Chanda<sup>1,2</sup>, Aditi Sen(De)<sup>1</sup>, Ujjwal Sen<sup>1</sup>

<sup>1</sup> *Harish-Chandra Research Institute, HBNI, Chhatnag Road, Jhansi, Allahabad 211 019, India and*

<sup>2</sup> *Instytut Fizyki im. Mariana Smoluchowskiego, Uniwersytet Jagielloński, Łojasiewicza 11, 30-348 Kraków, Poland.*

We report dynamical quantum phase transition portrait in the alternating field transverse XY spin chain with Dzyaloshinskii-Moriya interaction by investigating singularities in the Loschmidt echo and the corresponding rate function after a sudden quench of system parameters. Unlike the Ising model, the analysis of Loschmidt echo, analytically, yields non-uniformly spaced transition times in this model. Comparative study between the equilibrium and the dynamical quantum phase transitions in this case reveals that there are quenches where one occurs without the other, and the regimes where they co-exist. However, such transitions happen only when quenching is performed across at least a single gapless or critical line. Contrary to equilibrium phase transitions, bipartite entanglement measures do not turn out to be useful for the detection while multipartite entanglement emerges as a good identifier of this transition when the quench is done from a disordered phase of this model.

## I. INTRODUCTION

Quantum many body systems can undergo phase transition due to a variation in the system parameters at temperatures very close to absolute zero – entirely driven by quantum fluctuations [1]. Typically quantum critical points (QCPs) are identified by a vanishing energy gap and divergence in characteristic correlation lengths, thereby leading to singularities in physical quantities [2, 3]. For example, in recent years, bipartite as well as multipartite entanglement [4] have been proposed to be detectors of quantum phase transitions [5–7]. On the other hand, traditional or classical phase transitions (CPTs) are qualitatively different from quantum ones since the former is induced by thermal fluctuations.

Recent studies have shown that along with those in the equilibrium scenarios, quantum systems can also change their characteristics drastically by developing non-analyticities with time during their time evolution, such a phenomenon was named as dynamical quantum phase transition (DQPT), and is observed during the transient regime of evolution [8–11]. Specifically, the probability of a certain distance function between the initial and the final time-evolved states, known as Loschmidt echo [12], shows singularities with time, when the system lying initially in a particular phase of the underlying system, is typically quenched to a different phase. Extensive DQPT studies have been performed in one-dimensional quantum spin models like XY [13–21] and XXZ [22] models under different types of quenches [23], and several counter-intuitive results have been reported regarding the relation between the equilibrium quantum phase transition (EQPT) and DQPT [19, 24]. More importantly, DQPTs have been experimentally observed in trapped ions [25] where systems have been quenched from the ferromagnetic to the paramagnetic phase of the transverse field Ising model, while in another experiment, fermionic systems in a hexagonal lattice undergo a topological DQPT [26] (see also [27]). It is as yet not clear whether entanglement can be a useful and dependable physical quantity for detecting DQPTs. Some initial results in this direction indicate that vanishing Schmidt gap can be related to the zeroes of the Loschmidt echo [28] at critical times of the DQPT in the transverse field Ising spin chain. Apart from the

fundamental importance of such studies, with entanglement, it may have important implications in the design of quantum technologies like one-way and topological quantum computers and quantum simulators [29–34].

Towards finding the critical times, analytically, under general quenches and seeking the role of entanglement in DQPT, we consider here a uniform and alternating transverse field XY spin chain (ATXY) in presence of an additional antisymmetric interaction, the Dzyaloshinskii-Moriya (DM) interaction [35–68]. In equilibrium, the model displays several exotic phases which are not present in the XY spin chain, thereby, raising the possibility of having counter-intuitive observations in DQPTs in the generalized models. Since, analytical results for most general quenches such as a spin chain with an alternating transverse field, to our knowledge, have not yet been investigated in literature, we first find an analytical expression of Loschmidt echo for generalized quenches of the system parameters viz. the uniform field, the alternating field, and the DM interaction strength. We perform the analyses both for quenches within and across equilibrium phases, looking for criticalities in its time evolution as a way to establish a relation between EQPTs and DQPTs. We find that for quenches which involve both the uniform and alternating fields, there occur non-integer spaced critical times, in contrast to the uniformly spaced criticalities obtained for quenches involving only one of the two fields (the other being set to zero). Moreover, we find that DQPTs can occur even when quenching is done into the same phase [24]. Although, we notice that for DQPT to occur, there exists atleast a single gapless or critical line between initial and final variation in the system parameters. On top of that, there exist situations where even though the quench corresponds to a different equilibrium phase, DQPT does not occur [19].

Systematic studies reveal that if the initial state belongs to a disordered phase, multipartite entanglement can identify the presence of DQPT more efficiently, as compared to bipartite entanglement, except at the boundaries. Specifically, we observe that the time-averaged standard deviation of a geometric measure of multipartite entanglement [69] (see also [70–73]) detects the regions (in the system parameter space) corresponding to DQPT. These regions, obtained via analysis of

multipartite entanglement, show a large overlap with those detected through singularities in the Loschmidt echo.

The paper is organized as follows. We define and discuss the equilibrium phase diagram of the alternating field XY model with DM interaction (DATXY) model in Sec. II. The analysis of DQPT using Loschmidt amplitude is carried out in Sec. III. An analytical closed form expression of the rate function in the DATXY model is presented in Sec. III A. The non-analyticities of the rate function is analyzed in Sec. III B with the non-uniformly spaced critical times being computed in Sec. III B 1. The connection between dynamical and equilibrium quantum phase transitions are discussed in Sec. III B 2. The detection of DQPT via entanglement is carried out in Sec. IV, specifically with bipartite entanglement in Sec. IV A and with multipartite entanglement in Sec. IV B. Finally, a conclusion is presented in Sec. V.

## II. TRANSVERSE XY MODEL WITH ALTERNATING FIELD AND ANTI-SYMMETRIC INTERACTION

We consider a paradigmatic family of interacting quantum spin-1/2 systems on a one-dimensional (1D) lattice with nearest-neighbor anisotropic XY interaction as well as asymmetric Dzyaloshinskii-Moriya (DM) interaction in presence of uniform and alternating external transverse magnetic fields. The model is described by the Hamiltonian [35],

$$\hat{H} = \frac{1}{2} \sum_{j=1}^N \left[ J \left( \frac{1+\gamma}{2} \hat{\sigma}_j^x \hat{\sigma}_{j+1}^x + \frac{1-\gamma}{2} \hat{\sigma}_j^y \hat{\sigma}_{j+1}^y \right) + \frac{D}{2} (\hat{\sigma}_j^x \hat{\sigma}_{j+1}^y - \hat{\sigma}_j^y \hat{\sigma}_{j+1}^x) + (h_1 + (-1)^j h_2) \hat{\sigma}_j^z \right], \quad (1)$$

with periodic boundary condition, i.e.  $\hat{\sigma}_{N+1} = \hat{\sigma}_1$ . Here,  $\hat{\sigma}^\alpha, \alpha = x, y, z$  are the Pauli matrices,  $J$  and  $D$  represent the strengths of nearest-neighbor exchange interaction and the DM interaction respectively,  $\gamma (\neq 0)$  is the anisotropy parameter in the  $x - y$  direction,  $h_1$  and  $h_2$  are the uniform and alternating transverse magnetic fields respectively, and  $N$  denotes the total number of lattice-sites. We refer to this model as the DATXY model. The above Hamiltonian can be mapped to a spinless 1D Fermi system with two sublattices (for even and odd sites) via the Jordan-Wigner transformation [35, 74]. Further, performing Fourier transformation, the Hamiltonian can be block-diagonalized in the momentum space, as  $\hat{H} = \sum_{p=1}^{N/4} \hat{H}_p$ , with

$$\begin{aligned} \hat{H}_p = J & \left[ (\cos \phi_p + d \sin \phi_p) (a_p^\dagger b_p + b_p^\dagger a_p) \right. \\ & + (\cos \phi_p - d \sin \phi_p) (a_{-p}^\dagger b_{-p} + b_{-p}^\dagger a_{-p}) \\ & - i\gamma \sin \phi_p (a_p^\dagger b_{-p} + a_{-p} b_p - a_{-p}^\dagger b_p^\dagger - a_p b_p) \\ & + (\lambda_1 + \lambda_2) (b_p^\dagger b_p + b_{-p}^\dagger b_{-p}) \\ & \left. + (\lambda_1 - \lambda_2) (b_p^\dagger b_p + b_{-p}^\dagger b_{-p}) - 2\lambda_1 \right], \quad (2) \end{aligned}$$

where  $\lambda_i = h_i/J$  with  $i = 1, 2$  and  $d = D/J$  are the dimensionless system parameters,  $\phi_p = 2\pi p/N$ , and  $\hat{a}_p$  ( $\hat{b}_p$ )

correspond to the fermionic operators for odd (even) sublattices. Therefore, diagonalization of  $\hat{H}$ , required to study its characteristics, reduces in diagonalizing  $\hat{H}_p$  for different momentum sectors, which can be done by proper choice of the basis [35, 74].

It is noteworthy to mention that several well-known quantum spin models in different parameter regimes can be obtained from the DATXY model, such as

1. transverse field Ising (TFI) model for  $\gamma = 1, \lambda_2 = d = 0$ ,
2. quantum XY model with uniform magnetic field (UXY) for  $\lambda_2 = d = 0$ ,
3. quantum XY model with uniform and alternating magnetic fields (ATXY) [3, 74–77] for  $d = 0$ , and
4. quantum XY model with uniform magnetic field in presence of DM interaction (DUXY) for  $\lambda_2 = 0$ .

We choose the DATXY model for demonstration, as this model possesses a very rich phase diagram at zero temperature (see Fig. 1), with two paramagnetic phases (PM-I and PM-II), one antiferromagnetic phase (AFM), and one *gapless* chiral phase (CH). Moreover, we notice that by fixing different parameters suitably it can be reduced to any of the above four models. The equilibrium quantum phase transitions between these different phases occur across the following surfaces [35]:

- For  $0 \leq d < \gamma$ ,
  1.  $\lambda_1^2 = 1 + \lambda_2^2$  (PM-I  $\leftrightarrow$  AFM)
  2.  $\lambda_2^2 = \lambda_1^2 + \gamma^2 - d^2$  (PM-II  $\leftrightarrow$  AFM)
- For  $d > \gamma$ ,
  1.  $\lambda_1^2 = 1 + \lambda_2^2 + d^2 - \gamma^2$  (PM-I  $\leftrightarrow$  CH)
  2.  $\lambda_1 = \pm \lambda_2$  (PM-II  $\leftrightarrow$  CH).

Note that, in the thermodynamic limit, the AFM phase of the spin Hamiltonian given in Eq. (1) has two-fold degeneracy whereas, in the fermionic version of the model (i.e., Eq. (2)), the ground state in that phase is unique. The AFM phase appears for  $d < \gamma$ , whereas for  $d > \gamma$  we get the CH phase. The gapless CH phase, in addition of having a continuous spectra, has three-fold degenerate ground state.

## III. DYNAMICAL QUANTUM PHASE TRANSITIONS IN DATXY MODEL

Let us now set the stage for the investigation of dynamical quantum phase transitions (DQPT) in the DATXY model. In this paper, we consider the dynamics in the DATXY model, governed by a sudden quench of its parameters at time  $t = 0$ . Specifically, at  $t = 0$ , we prepare the system as a ground state of a Hamiltonian,  $\hat{H}^{(0)} = \hat{H}(g_0)$ , with initial parameter values,  $g_0 \equiv \{\lambda_1(t=0), \lambda_2(t=0), d(t=0)\}$ , and then at  $t > 0$ , we suddenly quench the system parameters to new

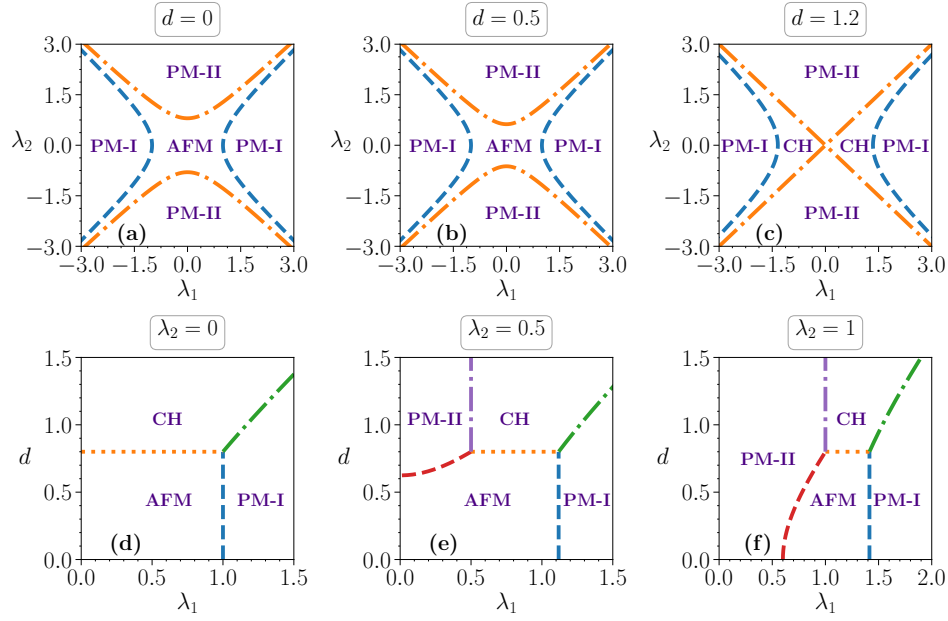


FIG. 1. (Color online.) Phase diagrams of the DATXY model in different parameter-spaces. Here, we choose  $\gamma = 0.8$ . Unless otherwise stated, we will use  $\gamma = 0.8$  throughout the paper for demonstration purpose. All quantities plotted are dimensionless.

values,  $g_1 \equiv \{\lambda_1(t > 0), \lambda_2(t > 0), d(t > 0)\}$ , such that the new Hamiltonian becomes  $\hat{H}^{(1)} = \hat{H}(g_1)$ , according to which the system evolves with time. Note that, unless otherwise stated, we will not change the anisotropy parameter,  $\gamma$ , in the quenching process.

### A. Loschmidt amplitude, Loschmidt echo

Analogous to the role of canonical partition function in temperature driven phase transitions, the Loschmidt amplitude is shown to play an important role in DQPTs [13, 14], and is defined as the overlap of the time evolved state of a system with its initial state. If the initial state,  $|\Psi^0\rangle$ , is prepared as the ground state of the initial Hamiltonian,  $\hat{H}^{(0)}$ , and the Hamiltonian after the quench is  $\hat{H}^{(1)}$ , then the Loschmidt amplitude is defined as

$$G(t) = \langle \Psi^0 | e^{-i\hat{H}^{(1)}t/\hbar} | \Psi^0 \rangle. \quad (3)$$

For quenching in the parameter-space of the DATXY model, using Eq. (2), the above expression can be decomposed as

$$G(t) = \prod_{p=1}^{N/4} \langle \Psi_p^0 | e^{-i\hat{H}_p^{(1)}t/\hbar} | \Psi_p^0 \rangle = \prod_{p=1}^{N/4} G_p(t), \quad (4)$$

where  $|\Psi_p^0\rangle$  is the eigenstate of  $\hat{H}_p^{(0)}$  corresponding to the lowest eigenvalue, and in the last expression, we have defined Loschmidt amplitude per momentum mode as  $G_p(t) = \langle \Psi_p^0 | e^{-i\hat{H}_p^{(1)}t/\hbar} | \Psi_p^0 \rangle$ . The Loschmidt echo,  $L(t)$ , is then described by the probability associated with this amplitude, i.e.,  $L(t) = |G(t)|^2$ . The rate function associated with  $L(t)$ , which

is analogous to the free energy (per lattice-site) in thermal phase transitions, can be defined as

$$\begin{aligned} \mathcal{F}(t) &= - \lim_{N \rightarrow \infty} \frac{1}{N} \log L(t) \\ &= - \lim_{N \rightarrow \infty} \frac{1}{N} \sum_{p=1}^{N/4} \log |G_p(t)|^2. \end{aligned} \quad (5)$$

Similar to the thermal phase transition, where transition is dictated by the nonanalytic behavior of the associated free energy with respect to the temperature, the DQPT can be detected by the nonanalyticity of the rate function as a function of time at some critical time  $t^*$ .

To deduce the analytical expressions of the Loschmidt amplitude and the rate function for a general quench from  $g_0 \equiv \{h_1(t=0), h_2(t=0), d(t=0)\}$  to  $g_1 \equiv \{h_1(t>0), h_2(t>0), d(t>0)\}$ , we introduce the fermionic vector operator

$\hat{A}_p = \begin{bmatrix} \hat{a}_p \\ \hat{b}_p \end{bmatrix}$ , such that we can write  $\hat{H}_p$  as follows:

$$\hat{H}_p = J \begin{bmatrix} \hat{A}_p^\dagger & \hat{A}_{-p}^\dagger \\ \hat{A}_p & \hat{A}_{-p} \end{bmatrix} \tilde{H}_p \begin{bmatrix} \hat{A}_p \\ \hat{A}_{-p} \end{bmatrix}, \quad (6)$$

with

$$\tilde{H}_p = \begin{bmatrix} (\cos \phi_p + d \sin \phi_p) \hat{\sigma}^x + \Lambda & -i\gamma \sin \phi_p \hat{\sigma}^x \\ i\gamma \sin \phi_p \hat{\sigma}^x & -(\cos \phi_p - d \sin \phi_p) \hat{\sigma}^x - \Lambda \end{bmatrix}, \quad (7)$$

where  $\Lambda = \text{Diag}\{\lambda_1 - \lambda_2, \lambda_1 + \lambda_2\}$ . To diagonalize  $\tilde{H}_p$  in Eq. (7), we can perform the Bogoliubov transformation,

$$\begin{bmatrix} \hat{A}_p \\ \hat{A}_{-p}^\dagger \end{bmatrix} = M_p \begin{bmatrix} \hat{\Gamma}_p \\ \hat{\Gamma}_{-p}^\dagger \end{bmatrix} = \begin{bmatrix} U_p & -iV_p \\ -iV_p^* & U_p^* \end{bmatrix} \begin{bmatrix} \hat{\Gamma}_p \\ \hat{\Gamma}_{-p}^\dagger \end{bmatrix}, \quad (8)$$

with  $\hat{\Gamma}_p = \begin{bmatrix} \hat{\eta}_p^a \\ \hat{\eta}_p^b \end{bmatrix}$ , such that  $\hat{H}_p$  is diagonal in the Bogoliubov basis,  $\{\hat{\eta}_p^{a\dagger}, \hat{\eta}_p^{b\dagger}, \hat{\eta}_{-p}^a, \hat{\eta}_{-p}^b\}$ . The fermionic algebra of  $\hat{a}_p, \hat{b}_p, \hat{\eta}_p^a$ , and  $\hat{\eta}_p^b$  operators guarantee that the Bogoliubov matrix,  $M_p$ , is unitary in nature, i.e.,  $M_p^{-1} = M_p^\dagger$ .

In order to calculate  $\langle \Psi^0 | e^{-i\hat{H}^{(1)}t/\hbar} | \Psi^0 \rangle$ , we need to express  $|\Psi^0\rangle$  in terms of Bogoliubov operators,  $\{\hat{\Gamma}_p(g_1)\}$ , that diagonalize  $\hat{H}^{(1)}$ . If the operators,  $\{\hat{\Gamma}_p(g_0)\}$ , diagonalize the initial Hamiltonian,  $\hat{H}^{(0)}$ , using Eq. (8), we arrive at the following relation:

$$\begin{aligned} \begin{bmatrix} \hat{\Gamma}_p(g_0) \\ \hat{\Gamma}_{-p}^\dagger(g_0) \end{bmatrix} &= M_p^{-1}(g_0) M_p(g_1) \begin{bmatrix} \hat{\Gamma}_p(g_1) \\ \hat{\Gamma}_{-p}^\dagger(g_1) \end{bmatrix}, \\ &= \begin{bmatrix} \mathcal{U}_p(g_0, g_1) & -i\mathcal{V}_p(g_0, g_1) \\ -i\mathcal{V}_p^*(g_0, g_1) & \mathcal{U}_p^*(g_0, g_1) \end{bmatrix} \begin{bmatrix} \hat{\Gamma}_p(g_1) \\ \hat{\Gamma}_{-p}^\dagger(g_1) \end{bmatrix}, \end{aligned} \quad (9)$$

with

$$\begin{aligned} \mathcal{U}_p(g_0, g_1) &= U_p^\dagger(g_0) U_p(g_1) + V_p^T(g_0) V_p^*(g_1), \\ \mathcal{V}_p(g_0, g_1) &= U_p^\dagger(g_0) V_p(g_1) - V_p^T(g_0) U_p^*(g_1). \end{aligned} \quad (10)$$

Calculation of  $\mathcal{U}_p$  and  $\mathcal{V}_p$  matrices entirely depend on the diagonalization of the  $4 \times 4$  matrices,  $\hat{H}_p(g_0)$  and  $\hat{H}_p(g_1)$ , in Eq. (7). Once the matrices,  $\mathcal{U}_p$  and  $\mathcal{V}_p$ , are obtained, we can write the initial state  $|\Psi^0\rangle$  as a boundary state composed of zero-momentum modes of  $\hat{H}^{(1)}$ , which is given by

$$|\Psi^0\rangle = \mathcal{N}^{-1} \exp \left[ i \sum_{p=1}^{N/4} \hat{\Gamma}_p^{\dagger T} (\mathcal{U}_p^{-1} \mathcal{V}_p) \hat{\Gamma}_{-p}^\dagger \right] |0\rangle, \quad (11)$$

where  $|0\rangle$  is the ground state of  $\hat{H}^{(1)}$ ,  $\mathcal{N}$  is the normalization constant, and  $T$  denotes the transpose of the corresponding

operators. If we now assume that operators  $\{\hat{\Gamma}_p(g_1)\}$  can diagonalize the Hamiltonian,  $\hat{H}^{(1)}$ , in the way, given by

$$\hat{H}_p^{(1)} = J \left[ \hat{\Gamma}_p^{\dagger T}(g_1) \quad \hat{\Gamma}_{-p}^T(g_1) \right] \begin{bmatrix} \hbar\omega_p^1 & 0 & 0 & 0 \\ 0 & \hbar\omega_p^2 & 0 & 0 \\ 0 & 0 & \hbar\omega_p^3 & 0 \\ 0 & 0 & 0 & \hbar\omega_p^4 \end{bmatrix} \begin{bmatrix} \hat{\Gamma}_p(g_1) \\ \hat{\Gamma}_{-p}^\dagger(g_1) \end{bmatrix}, \quad (12)$$

with  $\hbar\omega_p^k$ , for  $k = 1, 2, 3, 4$ , being the eigenvalues, then the Loschmidt amplitude,  $G(t) = \langle \Psi^0 | e^{-i\hat{H}^{(1)}t/\hbar} | \Psi^0 \rangle$ , reads as

$$\begin{aligned} G(t) &= \frac{e^{i\frac{Jt}{\hbar} \sum_{p=1}^{N/4} (\omega_p^3 + \omega_p^4)}}{\mathcal{N}^2} \langle 0 | \exp \left[ \sum_{p=1}^{N/4} \hat{\Gamma}_{-p}^T(g_1) M_p \hat{\Gamma}_p(g_1) \right] \\ &\quad \times \exp \left[ \sum_{p=1}^{N/4} \hat{\Gamma}_p^{\dagger T}(g_1) N_p \hat{\Gamma}_{-p}^\dagger(g_1) \right] |0\rangle, \end{aligned} \quad (13)$$

where

$$\begin{aligned} M_p &= \begin{bmatrix} -i\mathcal{T}_{11}^{p*} & -i\mathcal{T}_{21}^{p*} \\ -i\mathcal{T}_{12}^{p*} & -i\mathcal{T}_{22}^{p*} \end{bmatrix}, \\ N_p &= \begin{bmatrix} ie^{-i\frac{Jt}{\hbar}(\omega_p^1 - \omega_p^3)} \mathcal{T}_{11}^p & ie^{-i\frac{Jt}{\hbar}(\omega_p^1 - \omega_p^4)} \mathcal{T}_{12}^p \\ ie^{-i\frac{Jt}{\hbar}(\omega_p^2 - \omega_p^3)} \mathcal{T}_{21}^p & ie^{-i\frac{Jt}{\hbar}(\omega_p^2 - \omega_p^4)} \mathcal{T}_{22}^p \end{bmatrix}, \end{aligned} \quad (14)$$

with  $\mathcal{T}_{ij}^p = (\mathcal{U}_p^{-1} \mathcal{V}_p)_{ij}$ . Using Eqs. (13) and (14), and the prescription developed in [78], we get the Loschmidt amplitude per momentum mode for the DATXY model as

$$\begin{aligned} G_p(t) &= e^{i\frac{Jt}{\hbar}(\omega_p^3 + \omega_p^4)} \\ &\quad \times \frac{1 + e^{-i\frac{Jt}{\hbar}(\omega_p^1 - \omega_p^3)} |\mathcal{T}_{11}^p|^2 + e^{-i\frac{Jt}{\hbar}(\omega_p^2 - \omega_p^4)} |\mathcal{T}_{22}^p|^2 + e^{-i\frac{Jt}{\hbar}(\omega_p^1 - \omega_p^4)} |\mathcal{T}_{12}^p|^2 + e^{-i\frac{Jt}{\hbar}(\omega_p^2 - \omega_p^3)} |\mathcal{T}_{21}^p|^2 + e^{-i\frac{Jt}{\hbar}(\omega_k^1 + \omega_k^2 - \omega_k^3 - \omega_k^4)} |\mathcal{T}_{11}^p \mathcal{T}_{22}^p - \mathcal{T}_{12}^p \mathcal{T}_{21}^p|^2}{1 + |\mathcal{T}_{11}^p|^2 + |\mathcal{T}_{22}^p|^2 + |\mathcal{T}_{12}^p|^2 + |\mathcal{T}_{21}^p|^2 + |\mathcal{T}_{11}^p \mathcal{T}_{22}^p - \mathcal{T}_{12}^p \mathcal{T}_{21}^p|^2}, \end{aligned} \quad (15)$$

such that  $G(t) = \prod_{p=1}^{N/4} G_p(t)$ . Finally, we get the rate function associated with the quench from parameters  $g_0$  to  $g_1$ , in the thermodynamic limit, as

$$\mathcal{F}(t) = - \int_0^{\frac{\pi}{2}} \frac{d\phi_p}{\pi} \log |G_p(t)|. \quad (16)$$

**Note 1:** In case of quenching onto any phases of the ATXY model (i.e., for  $d(t > 0) = 0$ ), one can easily see that  $\omega_p^3 = -\omega_p^1$  and  $\omega_p^4 = -\omega_p^2$ , which simplify the form of  $G_p(t)$  in Eq. (15).

**Note 2:** The above treatment of Loschmidt amplitude and Loschmidt echo holds for non-degenerate initial ground state  $|\Psi^0\rangle$ . In case, the initial Hamiltonian,  $\hat{H}^{(0)} = \hat{H}(g_0)$ , has degenerate ground states, their definitions have to be generalized

(see Refs. [13–17]). To keep things simple, we will work with the fermionic version of the model, which is free from degeneracy in the AFM phase, and will not consider CH phase as the initial one since, the above analysis has to be modified in that situation. However, the final parameters of the quench in the  $(\lambda_1, \lambda_2, d)$  space, can belong to any phase.

## B. Nonanalyticity of the rate function

Let us analyze the rate function given in Eq. (16) for detecting DQPTs in the DATXY model for quenches across different points in the parameter space of the Hamiltonian.

Clearly, nonanalyticity arises in  $\mathcal{F}(t)$  (Eq. 16), if we can

find real solutions  $(\phi_p^*, t^*)$  of the transcendental equation

$$|G_p(t)| = 0, \quad (17)$$

which describes a DQPT with critical time  $t^*$ . As mentioned before, the matrix,  $\mathcal{T}$ , and the eigenvalues,  $\{\omega_p^k; k = 1, 2, 3, 4\}$ , can be computed easily by diagonalizing  $4 \times 4$  matrices,  $\tilde{H}_p(g_0)$  and  $\tilde{H}_p(g_1)$ , which, in turn, allows us to obtain  $G_p(t)$ , and thus the rate function,  $\mathcal{F}(t)$ .

For quenches in the the UXY model (i.e.,  $\lambda_2 = d = 0$ ), if the parameters of the model is changed from the PM-I phase to the AFM phase, or vice-versa (i.e., across  $\lambda_2 = 0$  line in Fig. 1(a)), one can get that  $\mathcal{T}_{12} = \mathcal{T}_{21} = 0$ . So, the expression for  $G_p(t)$  simplifies to the form, given by

$$G_p(t) = e^{-i\frac{Jt}{\hbar}(\omega_p^1 + \omega_p^2)} \frac{(1 + e^{-2i\frac{Jt}{\hbar}\omega_p^1} |\mathcal{T}_{11}^p|^2)(1 + e^{-2i\frac{Jt}{\hbar}\omega_p^2} |\mathcal{T}_{22}^p|^2)}{(1 + |\mathcal{T}_{11}^p|^2)(1 + |\mathcal{T}_{22}^p|^2)}. \quad (18)$$

The solutions of  $|G_p(t)| = 0$ , lead to critical times,  $t^*$  as

$$t^* = \frac{\hbar\pi}{J\omega_p^1} \left(n + \frac{1}{2}\right), \quad n = 1, 2, 3, \dots, \quad (19)$$

which matches with the known results of [13] for the TFI model. Note that the equation corresponding to  $\omega_p^2$  does not give any critical point. In case of  $\lambda_1 = d = 0$ , i.e., for quenching along the  $\lambda_1 = 0$  line in Fig. 1(a), we get similar expressions for  $t^*$ .

### 1. Non-uniformly spaced critical times

The DATXY model has a much richer phase diagram, as indicated by Fig. 1, compared to the UXY model, and hence we can anticipate some new features related to DQPTs, especially given the transcendental nature of Eq. (17). For example, in general, the critical times  $t^*$  are no longer uniformly spaced in the time-axis, which was the case for UXY or TFI model (Eq. (19)) [13]. For a general quench in the parameter-space of the DATXY model, the solutions of Eq. (17) are highly non-linear, unlike the previous UXY-scenario. In Fig. 2, we plot the rate function,  $\mathcal{F}(t)$  with  $t/t_1^*$ , where  $t_1^*$  is the first critical time, for quenches from the PM-I phase to AFM, PM-II, and CH phases respectively, such that all the quenches are performed across corresponding EQPT lines. Clearly, the critical times,  $t^*$ , are non-uniformly spaced across the time axis, as highlighted by normalizing the time axis to  $t/t_1^*$ .

### 2. Connection between DQPT and EQPT

For TFI model in 1D, it was found that DQPT are closely related to the EQPT [13, 14], which can be identified from the nonanalytic nature of the rate function being only observed for a quench across the EQPT line. However, later on, it was found that such relation no longer holds in the UXY model [19], as DQPT may occur for quenches in the same phase, or it may be absent for certain quenches into a different phase.

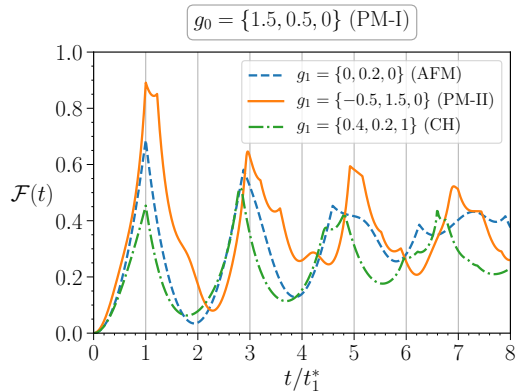


FIG. 2. (Color online.) Rate function,  $\mathcal{F}(t)$  vs.  $t/t_1^*$ . The dynamics occurs due to quenches from the point  $g_0 = \{1.5, 0, 0\}$ , which lies in the PM-I phase, to three different points, namely (1)  $g_1 = \{0, 0.2, 0\}$  (AFM phase), (2)  $g_1 = \{-0.5, 1.5, 0\}$  (PM-II phase), and (3)  $g_1 = \{0.4, 0.2, 1\}$  (CH phase), in the parameter-space of the DATXY model. All the quenches are across EQPT lines. Clearly, in all the three cases,  $\mathcal{F}(t)$  becomes nonanalytic for different critical times,  $t^*$ . Here, we have normalized the time-axis by the first critical time  $t_1^*$  in all the three cases to highlight the fact that in the DATXY model, the critical times are not uniformly spaced with each other. All quantities plotted are dimensionless.

In case of DATXY model, the situation is much more complicated. Below, we summarize our observations regarding the connections between DQPT and EQPT.

1. For  $d < \gamma$ , and quantum quenches from AFM phase to one of the PM phases, or vice-versa, DQPT has one-to-one correspondence with EQPT, i.e., DQPT can be observed if and only if quenching is performed into a different equilibrium phase (see Figs. 3 (a), (d)-(f)). However, if the anisotropy parameter,  $\gamma$ , is also quenched in the process, such connection no longer holds (see Ref. [19]).
2. The PM phases of DATXY model are connected by local transformations [75]. Therefore, one can expect that quenching between these two phases may not result to a DQPT. But our analysis shows that depending on the initial and final points in the parameter space of the DATXY model, a DQPT may, indeed, exist in case of quenching between these two PM phases (see Fig. 3(a)-(c), (f)). However, quenching between these phases not necessarily guarantees a DQPT. It is noteworthy to mention that PM-I and PM-II phases do not share a critical boundary, but separated by either AFM or CH phase (see Fig. 1).
3. For  $d > 0$ , a quench from a point in PM-II to another point in PM-II with different signs in  $\lambda_2$  may result into a DQPT (Fig. 3(c)). Although such quenches are performed into the same phase, another quantum phase (AFM or CH), and thus one or more gapless critical lines/regions have to be crossed in the quenching process, as the signs of initial and final  $\lambda_2$  are different.



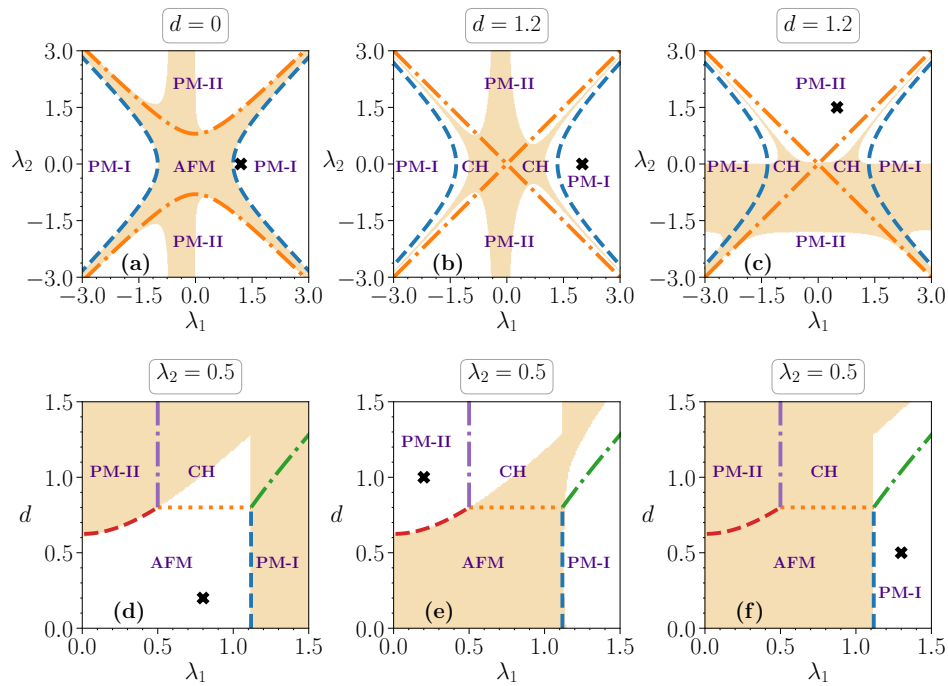


FIG. 3. (Color online.) DQPT regions in the parameter-space of the DATXY model for the quenches from the points marked by “ $\times$ ”. When a quantum quench is performed from a point, marked by the symbol “ $\times$ ”, to any other point on the parameter space, only the shaded region shows nonanalyticity in the rate function given in Eq. (16). In case of (a) the phase boundaries of Fig. 1(a) is taken, while for (b)-(c) and (d)-(f), the boundaries of Figs. 1(c) and Fig. 1(e) are chosen respectively. All the axes are dimensionless.

Note that this feature is special only to the PM-II phase, and can not be observed in any other phases for a fixed value of the anisotropy parameter,  $\gamma$ . Such observation is akin to the quench of  $\gamma$  as seen in Ref. [19].

4. For  $\lambda_2 = 0$  and fixed  $\lambda_1$ , quenching into the CH phase from the AFM phase by increasing  $d$  in the quantum quench does not result into a DQPT, as, in that case, the initial Hamiltonian,  $\hat{H}(\lambda_1, 0, d(< \gamma))$ , and the final Hamiltonian,  $\hat{H}(\lambda_1, 0, d(> \gamma))$ , commutes with each other. However, with  $\lambda_2 \neq 0$ , a DQPT from the AFM to CH phase is possible, provided the quenching is done sufficiently deep into the CH phase (Fig. 3(d)).
5. Similar to the quenching from the AFM to the CH phase, we report DQPT for certain situations when quenching have been performed from the PM-I or PM-II phase to well inside the CH phase (see Figs. 3(b), (c), (e) and (f)).

From the above observations, it is clear that, except for certain situations, there is no one-to-one connection between DQPT and EQPT phases in the DATXY model. However, all the observations reported here indicate that the *non analyticity of the rate function implies quench accross atleast a single critical line*.

In the next section, we would analyze DQPT from an information theoretic point of view involving both bipartite and multipartite entanglement, and compare it with the usual Loschmidt echo-based approach.

#### IV. CAN ENTANGLEMENT BE A POTENTIAL DETECTOR OF DQPT ?

In the case of equilibrium quantum phase transitions (EQPTs), entanglement, both bipartite as well as multipartite ones, emerged as efficient detectors [79]. It was shown that even in some models, EQPT could be detected by entanglement-based quantities where the traditional detection methods fail. For example, it was reported in [80] that for the spin-1 model proposed by Affleck, Lieb, Kennedy and Tasaki [81], EQPT was detected by a diverging entanglement-length in which the usual correlation lengths remain finite. Later, in other works [82–84], it was found that there exist models for which multipartite entanglement turns out to be better for identifying EQPT compared to bipartite measures. In a broader sense, it has been realized that nearest neighbour bipartite entanglement as well as other quantum correlation measures have the potential to uncover EQPTs that occur due to a change in system parameters. The question then is – Can entanglement be a “good” quantity to identify phase transitions that occur with the variation of time, after a sudden quench of parameters?

In this paper, we answer this question by analyzing the time evolution of bipartite and multipartite entanglement for the DATXY model after a sudden quench. Furthermore, we compare and contrast the DQPT detection capabilities of bipartite and multipartite entanglement and show multipartite entanglement to be a better identifier of DQPT compared to its bipartite counterparts.

### A. Bipartite entanglement

In this paper, we quantify bipartite entanglement via logarithmic-negativity,  $\mathcal{L}$ . For an arbitrary two party density matrix,  $\rho_{AB}$ , negativity ( $\mathcal{N}$ ) and  $\mathcal{L}$  are defined as

$$\begin{aligned}\mathcal{N}(\rho_{AB}) &= \frac{1}{2}(\|\rho_{AB}^{T_B}\| - 1) = \frac{1}{2}(\|\rho_{AB}^{T_A}\| - 1), \\ \mathcal{L}(\rho_{AB}) &= \log_2(2\mathcal{N}(\rho_{AB}) + 1),\end{aligned}\quad (20)$$

where  $\|A\| = \text{tr}\sqrt{A^\dagger A}$  and  $T_{A(B)}$  in the superscript of  $\rho_{AB}$  denotes partial transposition in party  $A(B)$ . Note that for  $2 \otimes 2$  and  $2 \otimes 3$  systems, negative partial transposition and hence non-zero  $\mathcal{L}$  provides a necessary and sufficient condition for guaranteeing entanglement [85]. Thus in our case, since all the two-site reduced density matrices have dimension  $2 \otimes 2$ ,  $\mathcal{L}$  is a faithful measure of entanglement.

Our analysis establishes that nearest neighbor entanglement shows some qualitative changes when a quench is performed across a disorder to order transition, i.e. PM-I (II)  $\rightarrow$  AFM/CH phase. Specifically, in these cases, the dynamics of  $\mathcal{L}$  displays a distinctive *collapse and revival* feature. On the other hand, if the final parameters of the quench correspond to a disordered phase which is same as the phase of the initial state,  $\mathcal{L}$  does not show any collapse or revival and simply oscillates with decreasing amplitude, finally reaching a steady value.

However, note that the above features are only general trends and there exist several counter-examples to these patterns. Further investigation reveals that the dynamics of  $\mathcal{L}$  shows a large overlap with the equilibrium phases and only has a weak connection with DQPT. Hence, we infer that bipartite entanglement is not an efficient detector of DQPT.

### B. Advantages of Multipartite Entanglement as a detector of DQPT

As mentioned earlier, along with bipartite entanglement, multipartite entanglement can also independently detect EQPT. In some cases, multipartite entanglement can even outperform the bipartite measures of entanglement in the sense that, for some models, the former can detect EQPT where the later fails to do so. In this section, we examine the DQPT detection capability of multipartite entanglement. For this investigation, we choose generalized geometric measure (GGM) as the measure of multipartite entanglement [69]. For a set of states which are non-genuinely multipartite entangled, denoted by  $nG$ , the GGM of a state  $|\psi\rangle$ , is defined by

$$\mathcal{G}(|\psi\rangle) = 1 - \max_{|\phi\rangle \in nG} |\langle \phi | \psi \rangle|^2, \quad (21)$$

which, for a  $N$ -party pure state, reduces to

$$\begin{aligned}\mathcal{G}(|\psi\rangle) &= 1 - \max\{\mu_{i_1:\text{rest}}^{\max}, \mu_{i_1 i_2:\text{rest}}^{\max}, \dots, \mu_{i_1 i_2 \dots i_M:\text{rest}}^{\max} | \\ & i_1, i_2 \dots i_M \in \{1, 2, \dots, \tilde{N}\}; i_k \neq i_l; k, l \in \{1, 2, \dots, M\}\},\end{aligned}\quad (22)$$

where  $\tilde{N} = N/2$  or  $(N-1)/2$  for even and odd lattice sizes respectively, and  $\mu^{\max}$  denotes the maximal eigenvalue of the

reduced density matrices with rank equal to the number of  $i$ 's present in the subscript of  $\mu$ . Therefore, the evaluation of GGM,  $\mathcal{G}(|\psi\rangle)$ , boils down to the evaluation of the maximum of maximal eigenvalues for all reduced density matrices.

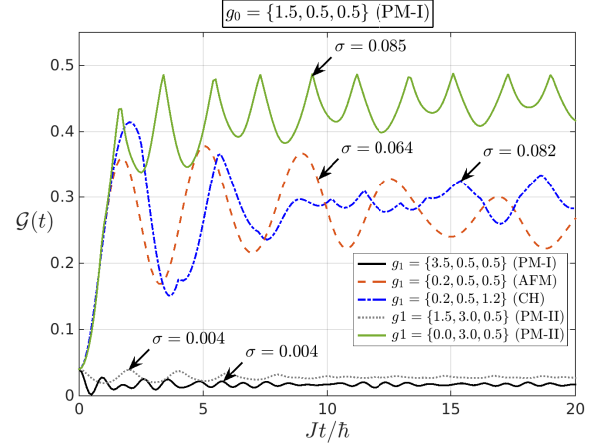


FIG. 4. (Color online) Time variation of  $\mathcal{G}$  after various quenches within and across equilibrium phases. We observe distinctly high amount of fluctuations during the transient period of dynamics for specific regions (corresponding to DQPT, see Fig. 3) of disorder to order (PM-I to AFM and PM-I to CH), and disorder to disorder (PM-I to PM-II) quenches, irrespective of the size of quench. Apart from these, other quenches show relatively lower fluctuations. Both the axes are dimensionless.

Although, the evaluation of GGM has a clear prescription, its computation requires finding the maximum eigenvalues of  $\binom{N}{1} + \binom{N}{2} + \dots + \binom{N}{N/2} \sim 2^N$  - number of matrices which is definitely cumbersome for large  $N$ . However, from finite size analysis of the DATXY model with  $N = 6, 8, 10$  and  $12$ , we notice that for almost all times (except the initial response time  $\sim \frac{2J}{\hbar}$ ), the maximal eigenvalue comes either from the single or nearest neighbour two-site reduced density matrices. So, we can argue that even for systems with large number of parties, the space consisting of the eigenvalues of single and nearest neighbour two-site reduced density matrices remain the *effective* subspace for computing the GGM. Furthermore, we can exploit the translational invariance of the DATXY model to simplify the scanning space even for the single and two-site reduced density matrices to just  $\rho_e, \rho_o, \rho_{eo}, \rho_{oe}$ . Here  $\rho_{e(o)}$  denotes the single site (reduced) density matrix corresponding to even and odd sites respectively, and  $\rho_{eo(oe)}$  is the nearest neighbour two-site density matrices between even-odd (odd-even) sites. Note that  $\rho_{eo}$  and  $\rho_{oe}$  have the same eigenvalues. Thus, in the thermodynamic limit ( $N \rightarrow \infty$ ), the GGM can be effectively computed as

$$\mathcal{G}(|\psi\rangle) \approx 1 - \max\{\mu_{\rho_e}^{\max}, \mu_{\rho_o}^{\max}, \mu_{\rho_{eo}}^{\max}\}, \quad (23)$$

Note that even if in some situations the above argument does not remain valid,  $\mathcal{G}(|\psi\rangle)$  still remains a measure of entanglement for multipartite states, providing an upper bound for GGM. Furthermore, it also remains an LOCC monotone.

We find that, multipartite entanglement,  $\mathcal{G}$  can capture DQPT when the quench corresponds to an underlying EQPT

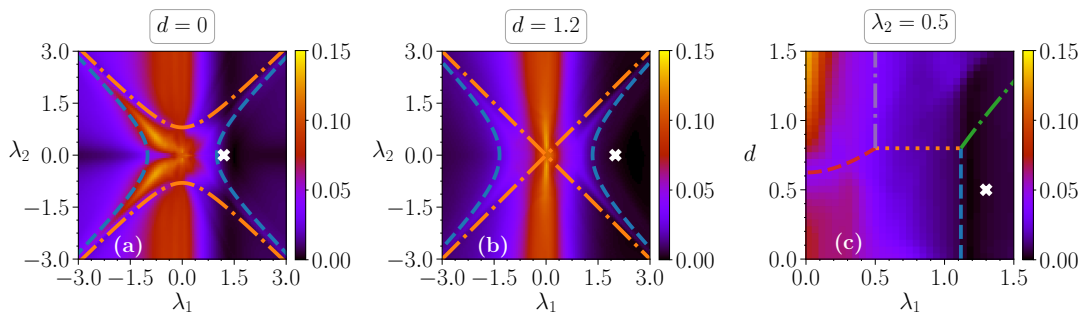


FIG. 5. (Color Online) Variation of time averaged standard deviation  $\langle \sigma_{\mathcal{G}}(t) \rangle$ , for quenches in  $(\lambda_1, \lambda_2, d)$ -space with initial choices indicated by “ $\times$ ” as in Fig. 3. After the quench, we observe the emergence of a specific region in the  $(\lambda_1, \lambda_2)$ -space in (a) and (b), and in  $(\lambda_1, d)$ -space in (c), which are distinctly characterized by a high fluctuations, i.e., higher values of  $\langle \sigma_{\mathcal{G}}(t) \rangle$ . This region possess a high overlap with that depicted in Fig. 3(a), (b) and (f), which correspond to DQPTs, obtained by analyzing non-analyticities in the rate function. This substantial overlap, establishes multipartite entanglement as a good detector of DQPT. All the axes are dimensionless.

involving a disorder to order (PM-I/II  $\rightarrow$  AFM/CH) or a disorder to disorder (PM-I(II)  $\rightarrow$  PM-II(I)) transition and is not solely dependent on the underlying EQPT as was the case for bipartite entanglement. In particular for a quench starting from the disordered phase, the dynamics of  $\mathcal{G}$  displays a higher amount of oscillations (see Fig. 4) for a quench that leads to a DQPT compared to other situations. For a quantitative treatment of the above observation, we estimate the amount of fluctuations in the time dynamics of  $\mathcal{G}$  during the transient regime, by computing its time averaged standard deviation,  $\langle \sigma_{\mathcal{G}}(t) \rangle$ , defined as

$$\langle \sigma_{\mathcal{G}}(t) \rangle = \frac{\hbar}{J\tau} \int_0^{\frac{J\tau}{\hbar}} \sigma_{\mathcal{G}}(t) dt, \quad (24)$$

where  $\sigma_{\mathcal{G}}^2(t) = (\mathcal{G}^2(t) - \langle \mathcal{G}(t) \rangle)^2$ . Note that for a reasonable average,  $\tau$  should be taken to be large, but, on the other hand, it should also be small enough so that the system does not reach to a steady state ( $\tau \leq \tau_{st}$  where  $\tau_{st}$  being the time when the system enters a steady state), ensuring that the average is computed in the transient regime. In our case, we choose  $\tau = 20$  (with  $\tau_{st} \sim 50$ ). We analyse the variation of  $\langle \sigma_{\mathcal{G}}(t) \rangle$  scanning the parameter space  $(\lambda_1, \lambda_2, d)$  of the DATXY model. It is evident from Figs. 5 (a), (b), (c) (compare with Fig. 3 (a), (b), (f) respectively) that the value of  $\langle \sigma_{\mathcal{G}}(t) \rangle$  increases substantially for quenches that correspond to a DQPT (depending on the initial choice of system parameters) It is stressed once again that this effect is not solely determined by the underlying EQPTs and is manifestly dependent on the presence or absence of DQPTs which is confirmed by a large overlap between the regions of DQPT as detected by singularities in the rate function and large oscillations in the dynamics of  $\mathcal{G}$  (compare Figs. 3 and 5).

To summarize, there exist regions of high  $\langle \sigma_{\mathcal{G}}(t) \rangle$ , detecting presence of DQPT, even when the quench parameters do not correspond to an underlying EQPT. Furthermore, we know that (via analysis using the rate function), even when the quench parameters correspond to an underlying EQPT, it might not necessarily lead to DQPT after the quench. Unlike bipartite entanglement, genuine multipartite entanglement can identify the absence of DQPT in these cases as reflected by

comparatively lower values of  $\langle \sigma_{\mathcal{G}}(t) \rangle$ . These features establish multipartite entanglement,  $\mathcal{G}$ , to be a *better* detector of DQPT.

Despite the advantages offered by multipartite entanglement, its DQPT detection capability is not ubiquitous. For example, if one starts from an ordered phase, the dynamics of  $\mathcal{G}$  cannot detect DQPT. Therefore, the time variation of multipartite entanglement considered here, can indicate the presence or absence of DQPTs only when the initial state parameters corresponds to a disordered phase.

## V. CONCLUSION

Dynamics of many body systems reveal qualitative differences depending on the initial and quenched values of system parameters – known as dynamical quantum phase transition (DQPT). Such transitions, as defined traditionally, pick out situations where the rate function associated with the Loschmidt echo displays non-analyticities after a quench of system parameters. Analysis of DQPT via the rate function reveals a weak connection between DQPT and the underlying quantum phase transition (EQPT) corresponding to the quench. Specifically, there exist scenarios where one occurs without the other, i.e., DQPT without EQPT and vice versa. However, our analysis strongly suggests that DQPT can only occur, if some gapless critical line/region is crossed during the quench [19].

In this work, the analysis of DQPT is carried out for the XY model in uniform or alternating transverse fields and with a Dzyaloshinskii-Moriya interaction when a quench is performed either in the magnetic fields or in the strength of DM interaction. Unlike Ising systems, in this case, we *analytically* found non-uniformly spaced critical times (as indicated by zeros of Loschmidt echo) for the quenches which correspond to a DQPTs. Taking motivations from the EQPT detection capability of entanglement, we test its prowess in the identification of DQPT. Our analysis establishes multipartite entanglement to be a good detector of DQPT in comparison to its bipartite analogs. Specifically, for our model, fluctuations of multipartite



tite entanglement in dynamics, efficiently identify DQPT for quenches starting from a disordered equilibrium phase.

The theory of DQPT, in essence, presents a quantitative formalism to understand the qualitative differences that occur during the dynamics of many body systems after quenching of system parameters. Being intrinsically a feature of the transient regime, the analysis of DQPT is also of practical importance since one does not have to wait until equilibration to observe the relevant physics. Recent experimental realization of DQPT in various physical systems further reinforces the

significance of such pragmatic studies.

## ACKNOWLEDGMENTS

This research was supported in part by the ‘IN-FOSYS scholarship for senior students’. Computational work for this study was carried out at the cluster computing facility in the Harish-Chandra Research Institute (<http://www.hri.res.in/cluster>).

- 
- [1] B. K. Chakrabarti, A. Dutta, and P. Sen, *Quantum Ising phases and transitions in transverse Ising models* (Springer Berlin Heidelberg, 1996).
- [2] S. Sachdev, *Quantum Phase Transitions* (Cambridge University Press, 2009).
- [3] S. Suzuki, J. Inoue, and B. K. Chakrabarti, *Quantum Ising Phases and Transitions in Transverse Ising Models* (Springer Berlin Heidelberg, 2013).
- [4] R. Horodecki, P. Horodecki, M. Horodecki, and K. Horodecki, *Rev. Mod. Phys.* **81**, 865 (2009).
- [5] L. Amico, R. Fazio, A. Osterloh, and V. Vedral, *Rev. Mod. Phys.* **80**, 517 (2008).
- [6] M. Lewenstein, A. Sanpera, V. Ahufinger, B. Damski, A. Sen(De), and U. Sen, *Advances in Physics* **56**, 243 (2007).
- [7] T. J. Osborne and M. A. Nielsen, *Phys. Rev. A*, **66** (2002).
- [8] A. Sen(De), U. Sen, and M. Lewenstein, *Phys. Rev. A* **72**, 052319 (2005).
- [9] K. Sengupta, S. Powell, and S. Sachdev, *Phys. Rev. A* **69**, 053616 (2004).
- [10] K. Sengupta, D. Sen, and S. Mondal, *Phys. Rev. Lett.* **100**, 077204 (2008).
- [11] A. Sen, S. Nandy, and K. Sengupta, *Phys. Rev. B* **94**, 214301 (2016).
- [12] A. Peres, *Quantum Theory: Concepts and Methods (Fundamental Theories of Physics Book 57)* (Springer, 2006).
- [13] M. Heyl, A. Polkovnikov, and S. Kehrein, *Phys. Rev. Lett.* **110**, 135704 (2013).
- [14] M. Heyl, *Rep. Prog. Phys.* **81**, 054001 (2018).
- [15] M. Heyl, *Phys. Rev. Lett.* **113**, 205701 (2014).
- [16] B. Žunkovič, M. Heyl, M. Knap, and A. Silva, *Phys. Rev. Lett.* **120**, 130601 (2018).
- [17] S. A. Weidinger, M. Heyl, A. Silva, and M. Knap, *Phys. Rev. B* **96**, 134313 (2017).
- [18] M. Heyl, *Phys. Rev. Lett.* **115**, 140602 (2015).
- [19] S. Vajna and B. Dóra, *Phys. Rev. B* **89**, 161105 (2014).
- [20] M. Heyl, *Phys. Rev. B* **95**, 060504 (2017).
- [21] M. Heyl and J. C. Budich, *Phys. Rev. B* **96**, 180304 (2017).
- [22] F. Andraschko and J. Sirker, *Phys. Rev. B* **89**, 125120 (2014).
- [23] D. M. Kennes, D. Schuricht, and C. Karrasch, *Phys. Rev. B* **97**, 184302 (2018).
- [24] F. Andraschko and J. Sirker, *Phys. Rev. B* **89**, 125120 (2014).
- [25] P. Jurcevic, H. Shen, P. Hauke, C. Maier, T. Brydges, C. Hempel, B. P. Lanyon, M. Heyl, R. Blatt, and C. F. Roos, *Phys. Rev. Lett.* **119**, 080501 (2017).
- [26] N. Fläschner, D. Vogel, M. Tarnowski, B. S. Rem, D.-S. Lühmann, M. Heyl, J. C. Budich, L. Mathey, K. Sengstock, and C. Weitenberg, *Nat. Phys.* **14**, 265 (2017).
- [27] X.-Y. Guo, C. Yang, Y. Zeng, Y. Peng, H.-K. Li, H. Deng, Y.-R. Jin, S. Chen, D. Zheng, and H. Fan, “Observation of dynamical quantum phase transition by a superconducting qubit simulation,” (2018), [arXiv:1806.09269](https://arxiv.org/abs/1806.09269).
- [28] E. Canovi, E. Ercolessi, P. Naldesi, L. Taddia, and D. Vodola, *Phys. Rev. B* **89**, 104303 (2014).
- [29] S. Bose, *Phys. Rev. Lett.* **91**, 207901 (2003).
- [30] T. J. Osborne and N. Linden, *Phys. Rev. A* **69**, 052315 (2004).
- [31] M. Christandl, N. Datta, A. Ekert, and A. J. Landahl, *Phys. Rev. Lett.* **92**, 187902 (2004).
- [32] R. Raussendorf and H. J. Briegel, *Phys. Rev. Lett.* **86**, 5188 (2001).
- [33] M. H. Freedman, A. Kitaev, M. J. Larsen, and Z. Wang, *Bulletin of the American Mathematical Society* **40**, 31 (2002).
- [34] I. M. Georgescu, S. Ashhab, and F. Nori, *Rev. Mod. Phys.* **86**, 153 (2014).
- [35] S. Roy, T. Chanda, T. Das, D. Sadhukhan, A. Sen(De), and U. Sen, [arXiv:1710.11037 \[quant-ph\]](https://arxiv.org/abs/1710.11037).
- [36] T. Moriya, *Phys. Rev.* **120**, 91 (1960).
- [37] T. Moriya, *Phys. Rev. Lett.* **4**, 228 (1960).
- [38] P. W. Anderson, *Phys. Rev.* **115**, 2 (1959).
- [39] T. Siskens, H. Capel, and K. Gaemers, *Physica A* **79**, 259 (1975).
- [40] T. Siskens and H. Capel, *Physica A* **79**, 296 (1975).
- [41] J. Perk and H. Capel, *Phys. Lett. A* **58**, 115 (1976).
- [42] J. Perk and H. Capel, *Physica A: Statistical Mechanics and its Applications* **92**, 163 (1978).
- [43] O. Derzhko, T. Verkholyak, T. Krokhmalkii, and H. Büttner, *Phys. Rev. B* **73**, 214407 (2006).
- [44] K. Maruyama, T. Iitaka, and F. Nori, *Phys. Rev. A* **75**, 012325 (2007).
- [45] R. Jafari, M. Kargarian, A. Langari, and M. Siahatgar, *Phys. Rev. B* **78**, 214414 (2008).
- [46] S. Chuan-Jia, C. Wei-Wen, L. Tang-Kun, H. Yan-Xia, and L. Hong, *Chin. Phys. Lett.* **25**, 817 (2008).
- [47] R. Jafari and A. Langari, [arXiv:0812.1862 \[cond-mat.str-el\]](https://arxiv.org/abs/0812.1862).
- [48] M. Kargarian, R. Jafari, and A. Langari, *Phys. Rev. A* **79**, 042319 (2009).
- [49] W. W. Cheng and J.-M. Liu, *Phys. Rev. A* **79**, 052320 (2009).
- [50] X. S. Ma and A. M. Wang, *Opt. Commun.* **282**, 4627 (2009).
- [51] J. H. H. Perk and H. Au-Yang, *J. Stat. Phys.* **135**, 599 (2009).
- [52] C. Yi-Xin and Y. Zhi, *Commun. Theor. Phys.* **54**, 60 (2010).
- [53] X. Hao, *Phys. Rev. A* **81**, 044301 (2010).
- [54] Z. Kádár and Z. Zimborás, *Phys. Rev. A* **82**, 032334 (2010).
- [55] B.-Q. Liu, B. Shao, J.-G. Li, J. Zou, and L.-A. Wu, *Phys. Rev. A* **83**, 052112 (2011).
- [56] A. Das, S. Garnerone, and S. Haas, *Phys. Rev. A* **84**, 052317 (2011).

- [57] B. Li, S. Y. Cho, H.-L. Wang, and B.-Q. Hu, *J. Phys. A: Math. Theor.* **44**, 392002 (2011).
- [58] F.-W. Ma, S.-X. Liu, and X.-M. Kong, *Phys. Rev. A* **84**, 042302 (2011).
- [59] Y. Yan, L. Tian, and L. Qin, [arXiv:1109.5458 \[quant-ph\]](https://arxiv.org/abs/1109.5458).
- [60] R. Jafari and A. Langari, *Int. J. Quant. Info.* **09**, 1057 (2011).
- [61] J. Vahedi and S. MahdaviFar, *Euro. Phys. J. B* **85**, 171 (2012).
- [62] W. S. Cole, S. Zhang, A. Paramekanti, and N. Trivedi, *Phys. Rev. Lett.* **109**, 085302 (2012).
- [63] H. T. Wang and S. Y. Cho, [arXiv:1310.3169 \[cond-mat.str-el\]](https://arxiv.org/abs/1310.3169).
- [64] E. Mehran, S. MahdaviFar, and R. Jafari, *Phys. Rev. A* **89**, 042306 (2014).
- [65] M. Soltani, J. Vahedi, and S. MahdaviFar, *Physica A* **416**, 321 (2014).
- [66] G.-H. Liu, W.-L. You, W. Li, and G. Su, *J. Phys.: Cond. Matt.* **27**, 165602 (2015).
- [67] W. Chen and M. Sigrist, *Phys. Rev. Lett.* **114**, 157203 (2015).
- [68] K. K. Sharma and S. N. Pandey, *Quant. Info. Process.* **15**, 4995 (2016).
- [69] A. Sen(De) and U. Sen, *Phys. Rev. A* **81**, 012308 (2010).
- [70] A. Shimony, *Annals of the New York Academy of Sciences* **755**, 675 (1995).
- [71] H. Barnum and N. Linden, *J. Phys. A: Mathematical and General* **34**, 6787 (2001).
- [72] T.-C. Wei and P. M. Goldbart, *Phys. Rev. A* **68**, 042307 (2003).
- [73] M. Blasone, F. Dell'Anno, S. De Siena, and F. Illuminati, *Phys. Rev. A* **77**, 062304 (2008).
- [74] T. Chanda, T. Das, D. Sadhukhan, A. K. Pal, A. Sen(De), and U. Sen, *Phys. Rev. A* **94**, 042310 (2016).
- [75] U. Divakaran, A. Dutta, and D. Sen, *Phys. Rev. B* **78**, 144301 (2008).
- [76] S. Deng, L. Viola, and G. Ortiz, in *Recent Progress in Many-Body Theories* (World Scientific, 2008) [arXiv:0802.3941 \[cond-mat.stat-mech\]](https://arxiv.org/abs/0802.3941).
- [77] A. Dutta, G. Aeppli, B. K. Chakrabarti, U. Divakaran, T. F. Rosenbaum, and D. Sen, *Quantum Phase Transitions in Transverse Field Spin Models: From Statistical Physics to Quantum Information* (Cambridge University Press, 2015).
- [78] A. LeClair, G. Mussardo, H. Saleur, and S. Skorik, *Nucl. Phys. B* **453**, 581 (1995).
- [79] L.-A. Wu, M. S. Sarandy, and D. A. Lidar, *Phys. Rev. Lett.* **93**, 250404 (2004).
- [80] F. Verstraete, M. A. Martín-Delgado, and J. I. Cirac, *Phys. Rev. Lett.* **92**, 087201 (2004).
- [81] I. Affleck, T. Kennedy, E. H. Lieb, and H. Tasaki, *Comm. Math. Phys.* **115**, 477 (1988).
- [82] A. Biswas, R. Prabhu, A. Sen(De), and U. Sen, *Phys. Rev. A* **90**, 032301 (2014).
- [83] R. W. Chhajlany, P. Tomczak, A. Wójcik, and J. Richter, *Phys. Rev. A* **75**, 032340 (2007).
- [84] M. N. Bera, R. Prabhu, A. Sen(De), and U. Sen, [arXiv:1209.1523 \[quant-ph\]](https://arxiv.org/abs/1209.1523).
- [85] M. Horodecki, P. Horodecki, and R. Horodecki, *Phys. Lett. A* **223**, 1 (1996).